

Tuning the Emission Behaviour of Halogenated Bridged Ethers in Solution, as Solids and as Aggregates by Chalcogen Substitution

Justin Dubbert⁺,^[a] Marco Valtolina⁺,^[e] Alexander Huber,^[a] Tim D. Scherz,^[a] Christoph Wölper,^[b] Constantin G. Daniliuc,^[c] Ofer Filiba,^[d] Saumik Sen,^[d, g] Igor Schapiro,^[d] Fabio Rizzo,^{*,[e, f]} and Jens Voskuhl^{*,[a]}

In this contribution, we describe a set of three chlorinated bridged ethers with varying numbers of sulfur and oxygen atoms. The substitution leads to highly emissive compounds with tunable photophysical properties in relationship to their state of aggregation, i.e. in solution, as aggregates and in the solid state. Additionally, an in-depth X-ray diffractometric

analysis supported by a Hirshfeld study of non-covalent interactions and quantum chemical simulations was carried out. As the outcome, it was found that the content of sulfur in the compounds regulates the tuning of emission in solution as well as in the aggregated states as a consequence of their variation of planarity.

Introduction

Fluorescence, the emission from an excited singlet state, is used in many technological applications ranging from materials science^[1] to biological imaging.^[2] Regardless of the desired application, the tuning of the emission behaviour in different physical conditions, namely, solid, crystalline, aggregated or dissolved state remains a challenging task. Especially the influence of these conditions on the emission properties of purely organic compounds inspired numerous groups around the world to shine light on this issue, which was highlighted in numerous reviews.^[3] Classic luminophores such as polyaromatic compounds including rhodamine,^[4] fluorescein^[5] or condensed aromatics^[6] are known to emit brightly dissolved in solution, whereas quenching in the solid and aggregated state is observed, due to non-radiative decay pathways, including unfavourable π - π -contacts. This effect known as aggregation-caused quenching (ACQ) leads to a restriction of applications in the condensed state. The opposite effect occurs when flexible, non-planar and in its motion free organic luminophores are used instead of molecularly rigid structures. In this case the emission is typically observed in the solid and aggregated state besides a non-radiative decay in the dissolved molecule, which is typically attributed to a conversion of absorbed light into motion. The hindrance of this flexibility, e.g. in the bound, condensed or crystalline state leads to an opening of radiative decay channels taking into account the non-planar structure of these twisted compounds in the solid-state.^[7] This phenomenon is known since decades,^[3d] has been described for “solid solutions” around 100 years ago^[8] and has experienced a renaissance when scientists discovered that propeller-like methyl-pentaphenylsiloles show emission only when aggregated or in the solid-state.^[9] The term aggregation-induced emission (AIE),^[3a,10] which is typically used for this phenomenon, has attracted interest in the past two decades, but is somewhat

[a] J. Dubbert,⁺ A. Huber, T. D. Scherz, Prof. J. Voskuhl
Faculty of Chemistry (Organic Chemistry)
ZMB and Center for Nanointegration (CENIDE)
University of Duisburg-Essen
Universitätsstrasse 7, 45117 Essen (Germany)
E-mail: jens.voskuhl@uni-due.de

[b] Dr. C. Wölper
Faculty of Chemistry (Inorganic Chemistry)
University of Duisburg-Essen
Universitätsstrasse 7, 45117 Essen (Germany)

[c] Dr. C. G. Daniliuc
Organisch-Chemisches Institut
Westfälische Wilhelms-Universität
Corrensstraße 36, 48149 Münster (Germany)


[d] O. Filiba, Dr. S. Sen, Prof. Dr. I. Schapiro
Fritz Haber Center for Molecular Dynamics Research
Institute of Chemistry
The Hebrew University of Jerusalem
9190401 Jerusalem (Israel)


[e] M. Valtolina,⁺ Dr. F. Rizzo
Center for Soft Nanoscience (SoN)
Westfälische Wilhelms-Universität Münster
Busso-Peus-Str. 10, 48149 Münster (Germany)

[f] Dr. F. Rizzo
Institute of Chemical Science and Technologies “G. Natta” (SCITEC)
National Research Council (CNR)
Via G. Fantoli 16/15, 20138 Milan (Italy)
E-mail: fabio.rizzo@cnr.it

[g] Dr. S. Sen
Present address:
Condensed Matter Theory Group, Laboratory for Theoretical and Computational Physics
Paul Scherrer Institute
CH-5232 Villigen PSI (Switzerland)

[⁺] These authors contributed equally to this work.

 Supporting information for this article is available on the WWW under <https://doi.org/10.1002/cptc.202200169>

 © 2022 The Authors. ChemPhotoChem published by Wiley-VCH GmbH. This is an open access article under the terms of the Creative Commons Attribution Non-Commercial License, which permits use, distribution and reproduction in any medium, provided the original work is properly cited and is not used for commercial purposes.

misleading, since not only aggregates show an emission “on” behaviour, but also a single molecule, when sterically entrapped in a demanding environment, such as a gel^[11] or viscous solution,^[12] a protein pocket^[13] or a polymer.^[14] These compounds typically featuring phenyl-rotors, have been used to fabricate reporter molecules for bioimaging,^[15] luminescent polymeric materials^[16] as well as organic light emitting diodes.^[17]

In between these two phenomena, a rational design concept combining both emissive properties appeared improbable since the molecular aspects of rigid planar structures (ACQ) and twisted movable moieties (AIE) seemed contradictory.^[18] Although some observations were published by Patra et al. in 2007 and by Tang et al. in 2012,^[19] compounds exhibiting emission in both solid and molecular states were first denoted as “dual-state efficient” (DSE) luminophores in 2015.^[20] Later, this effect describing compounds emitting light independently from the state of aggregation^[21] was labelled as “dual-state emission”. It is noteworthy, that this does not imply emission from different electronic states^[22] (i.e. singlet and triplet), but is solely based on the aggregation state.^[23] Hence, to avoid confusion, the term “solution and solid-state emitters” (SSSE) will be used in this contribution.^[24]

Since 2015, reports featuring compounds exhibiting the novel SSSE phenomenon have increased gradually. Several research groups investigated known luminescent key structural motifs for SSSE such as triphenylamines,^[25] carbazoles^[26] or pyrroles.^[27] Recently, Rodríguez-Molina and co-workers published a comprehensive review of reported SSSEs categorized by their respective structural units.^[21] Although some modular design concepts such as self-isolation^[28] or stacking modulation have been developed, more intrinsically oriented strategies to obtain SSSEs remain a challenging task.

In this context subtle variations of the molecular structure of a compound class were described to change the photophysical properties in different states of aggregation. Lately, we were able to describe AIE and SSSE^[24] based on either aromatic thioethers^[29] or bridged oxo- and thioethers.^[30] Although libraries of these compounds were investigated bearing different chalcogens or functional groups, only one effect (either SSSE or AIE) was observed. Wang et al. described in 2018 that diarylmaleimide-based luminophores featuring a benzofuran or benzothiophene moiety can be tuned regarding their emission properties by subtle molecular changes, such as substitution pattern and chalcogen variation. In this regard, they were able to obtain all three potential emission scenarios including SSSE, ACQ and AIE.^[31a] Both described oxygen containing compounds emit independently of their state of aggregation, which was attributed to the formation of *J*-aggregates in the solid-state and weak intermolecular interactions. Interestingly, the sulfur-containing derivatives either emit in the solid state or in solution, which was explained by motional freedom in solution (no emission) or the formation of hydrogen networks in the solid-state (no emission). Feng et al. reported three thioether based isomers showing different behaviour in emission in solution and solid state (either phosphorescence or SSSE) depending on the position of the sulfur and oxygen atoms.^[31b]

However, they hypothesized AIE as cause of the solid state emission without discussing the phenomenon of reprecipitation in organic solvent/water mixtures, which is useful to understand the occurrence of the ACQ, AIE and SSSE phenomena. Xiang et al. reported on the synthesis of salicylaldehyde azines that can also be tuned regarding their emission in dependency of their state of aggregation, and were found to be highly dependent on the substituent.^[32] In particular, most compounds revealed AIE behaviour, whereas the compounds bearing a $-\text{NEt}_2$ could also be regarded as SSSE, due to the bulkier residues hindering the packing induced self-quenching and rotation in solution.

By aiming to expand the knowledge of compounds showing AIE and SSSE behaviour, in this contribution three compounds based on chlorinated bridged ethers bearing sulfur and/or oxygen as chalcogens were investigated regarding their emission properties as well the influence of the state of aggregation on the photophysical properties (Figure 1).

Results and Discussion

The three compounds (O_2), (SO) and (S_2) were synthesized according to a modified protocol from the literature and have been used in a previous study as unexplored precursor compounds.^[24] The synthesis was carried out starting from tetrachlororephthalonitrile, which reacted under basic conditions with one equivalent of catechol, benzen-1,2-dithiol or 2-hydroxythiophenol yielding the desired compounds in good to acceptable yields (See Supporting Information for experimental details). All three compounds revealed striking emission properties in solution and in the solid-state, with a concomitant redshift upon replacing stepwise oxygen by sulfur atoms.

X-ray diffractometric and Hirshfeld analyses

The compounds were obtained as crystalline material, suitable for X-ray diffraction (Figure 2 and S1–S16).^[42] S_2 crystallizes in the monoclinic space group $P2_1/c$ with one independent molecule in the asymmetric unit. For O_2 the orthorhombic space group $Pcca$ was found with the molecule located on a two-fold rotational axis. SO is triclinic with space group $P-1$ where the molecule is placed on the general position. All three packings share the same ring motif of two $\text{CN}\cdots\text{Cl}$ interactions (see Figure S4, S9 and S15) leading to zig-zag chains. These chains interlock in a zipper-like way and are connected by $\text{CH}\cdots\text{N}$ hydrogen bonds to form a layer (side view in Figure S5,

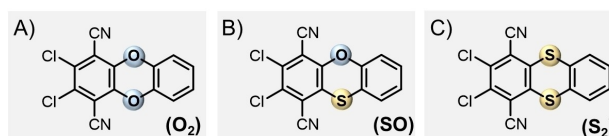


Figure 1. Molecular structure of A) (O_2), B) (SO) and C) (S_2).

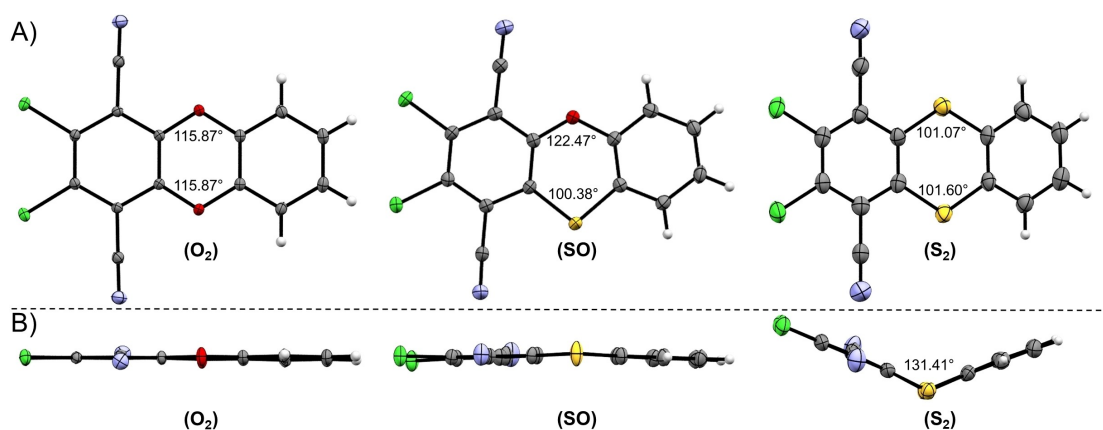


Figure 2. X-ray diffractometric analyses of O_2 , SO and S_2 in front view and side view including relevant bonding angles. Hydrogen atoms are omitted for clarity. Thermal ellipsoids are shown with 30% (S_2) or 50% (O_2 and SO) of probability. CCDC: S_2 (2164566), O_2 : (2164859), SO : (2164860).^[42]

S10 and S16). In S_2 and O_2 the layers are corrugated. In SO , due to the different length of the C–O and C–S bond, the position of the non-substituted ring is slightly rotated leading to different CH...N hydrogen bonds. Here the one donor atom is *ortho* and the other *meta* to the hetero atom instead of twice *meta*. Also an additional CH...Cl hydrogen bond is observed. The layers are interconnected by interactions of the π -systems (Figures S3, S8 and S14). In SO interactions between the phenyl-rings and others between the π -systems of the nitrile groups can be found. A tilt of the molecules in O_2 leads to CN... π (nitrile) instead of the π ... π interactions between the nitrile groups (Figure S11). In S_2 the angle in the molecule (Figure 2 and S1) leads to a neat stacking of the molecules allowing π ... π and S... π interactions (Figure S3).

The presence of various interactions in the layers of these compounds were further studied using quantum chemical calculations (Figure S22 and Table S10). The interaction energies were calculated in dimers using Symmetry Adapted Perturbation Theory (SAPT) and are shown in Table S11. Among three compounds, the S_2 dimer possesses the highest stabilization energy mainly due to the presence of several intermolecular interactions.

Since these non-covalent interactions are known to influence the photophysical parameters in the neat crystalline and microcrystalline state, we investigated those interactions by a Hirshfeld analysis using Crystal Explorer.^[33] This approach enables a quantitative evaluation of the corresponding non-covalent interactions within the crystal lattice, using d_i (distance internal) and d_e (distance external) under the formation of a d -norm surface.

Since numerous interactions have been found (Figure S17–S20 and Table S4), we wish to focus on the main interactions that are known to influence the optical properties in the solid-state such as C–H... π (indicated by C–H), π ... π (indicated by C–C), S... π (indicated as S–C) and Van der Waals interactions (indicated by H–H) (Table S4 and Figure S20). When comparing all three compounds regarding these specific interactions, it was found that SO and S_2 reveal significantly higher contributions of π -contacts when compared with O_2 , which showed a

significant contribution of CN... π interactions (Figure S11). This tilted parallel stacking of O_2 results in a higher fluorescence quantum efficiency (Φ_{PL}) in the solid-state compared to SO (Table 1), because unfavourable π -contacts are prevented, which would enable non-radiative decay. Interestingly, the highest quantum yield was determined for S_2 , which can be attributed to different specific features of non-covalent interactions and packing patterns. Although a significant contribution of π - π interactions were found, the C–S–C angle of 131.4° in S_2 leads to a drastic deviation from planarity featuring numerous C...S contacts (Figure S3), which prevents planar disc-like stacking (compare with Figure S8 and S14), leading to enhanced PLQY in the solid state.

Emission behaviour in the molecularly dissolved state

To get a deeper insight into the spectroscopic features of the three compounds, steady state emission spectra as well as time-resolved photoluminescence decays (τ) in solution and the solid state were performed (Table 1). The three molecules (O_2), (SO) and (S_2) have been reported previously as intermediate compounds for the preparation of expanded aromatic systems,^[24] but their photophysical properties have not been reported yet. Therefore, we provide a systematic comparison of the dyes to understand how the variation of sulfur and oxygen content affects their photophysics.

All luminophores show very similar absorption bands in dichloromethane (DCM) with peak maxima around 390–410 nm (Figure 3) with extinction coefficient ϵ of 7100, 4580, and 3650 $\text{cm}^{-1} \text{M}^{-1}$ for O_2 , SO and S_2 , respectively.

The replacement of oxygen by sulfur in SO and S_2 induces a bathochromic shift of the absorption band compared to O_2 , suggesting a conjugation effect connected with the electronic features of sulfur (low electronegativity and high π -polarizability). However, while the effect on the absorption maximum is rather small, the shift of the fluorescence maximum is significantly larger. Introducing sulfur atoms changes the geometry but also the electronic structure of the luminophore.

Table 1. Overview of the photophysical parameters of (O_2), (SO) and (S_2) measured in different solvents and in the solid state.

Compound	Solvent	Polarity index	λ_{abs} [nm]	λ_{em} [nm]	Stokes shift [nm/cm ⁻¹]	τ [ns]	Φ_{PL} [%] ^[b]	k_r [10 ⁷ s ⁻¹]	k_{nr} [10 ⁷ s ⁻¹]
O_2	Cyclohexane	0.006	391	432	41/2427	0.74	7	9.46	125.68
	Toluene	0.099	388	457	69/3891	2.49	20	8.03	32.13
	Chloroform	0.259	391	463	72/3977	3.41	26	7.62	21.70
	DCM	0.309	390	464	74/4089	3.77	25	6.63	19.89
	DMF	0.386	390	513	123/6148	2.68 ^[a]	2	0.75	36.57
	ACN	0.460	386	490	104/5499	1.02	6	5.88	92.16
	Solid-state	-	370 ^[c]	464	94/5475	1.88 ^[a]	16	8.51	44.68
SO	Cyclohexane	0.006	400	465	65/3495	1.08	7	6.48	86.11
	Toluene	0.099	408	506	98/4747	3.88	17	4.38	21.39
	Chloroform	0.259	411	509	98/4685	3.40	22	6.47	22.94
	DCM	0.309	411	514	103/4876	3.74	21	5.61	21.12
	DMF	0.386	409	523	114/5329	3.64 ^a	47	12.91	14.56
	ACN	0.460	405	540	135/6173	3.66	17	4.64	22.68
	Solid-state	-	430 ^[c]	516	86/3876	3.23	14	4.33	26.63
S_2	Cyclohexane	0.006	390	508	118/5956	1.01	5	4.95	94.06
	Toluene	0.099	393	551	158/7296	2.11	9	4.27	43.13
	Chloroform	0.259	397	556	159/7203	2.56	11	4.30	34.77
	DCM	0.309	395	563	168/7554	2.98	11	3.69	29.87
	DMF	0.386	410	570	160/6846	7.60 ^[a]	30	3.95	9.21
	ACN	0.460	390	577	187/8310	3.17	10	3.15	28.39
	Solid-state	-	460 ^[c]	556	96/3754	337.11 μ s ^[a]	40	1187 s ⁻¹	1780 s ⁻¹

[a] Biexponential fitting; [b] Measured by integrating sphere with an error of $\pm 2\%$; [c] From the excitation spectrum.

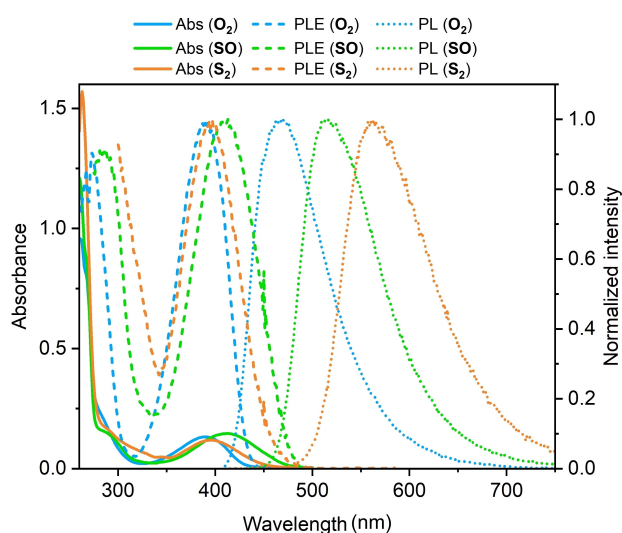


Figure 3. Absorption (full lines), excitation (PLE, dashed lines) and emission (PL, dotted lines) spectra of O_2 (16 μ M, blue lines), SO (38 μ M, green lines) and S_2 (23 μ M, orange lines) in dichloromethane. The PLE and PL spectra are normalized for comparison.

Hence, it is difficult to disentangle these effects to explain the shift in absorption versus the shift in emission maxima. Instead we focused the analysis on the change in the Stokes shift, because it can be rationalized by the extend of geometrical changes between the ground and excited state geometries. The increasing content of bridging sulfur is leading to a larger geometrical change in the excited state, which strongly correlates with the shift of the emission maximum of the fluorophores. We observed that the relaxation in the excited state leads to a more planar geometry in SO and S_2 . The change in the bending of the molecular plane (Figure 6) is

increasing from 0 to 16.6° and to 22.9° for O_2 , SO and S_2 , respectively. This suggests that a larger relaxation in the excited state lowers the energy gap between the S_0 and S_1 states, leading to a larger Stokes shift.

Noteworthy, in SO the absorption band is more red-shifted than in S_2 (411 nm vs. 395 nm, respectively) whereas the emission shows the opposite behaviour (514 nm vs. 563 nm, respectively), suggesting that the asymmetric structure affects more the ground state than the excited state. The short lifetime values recorded in DCM (around 3 ns for all three compounds) indicate radiative processes through fluorescence, with average fluorescence rate constants (k_r) and the corresponding non-radiative deactivation rates (k_{nr}) on the same order of magnitude (Table 1). Interestingly, in DCM the fluorescence quantum efficiency (Φ_{PL}) of S_2 (11 %) is significantly lower than O_2 (25 %) and SO (21 %).

By investigating the photophysical properties in different solvents, we observed that the absorption band of O_2 is almost not affected by the solvent polarity, whereas slightly higher shifts are noticed in both SO and S_2 (Figure S23, S24). The emission bands of the three dyes are more affected by the change of the polarity, showing a positive solvatochromism that suggests a more polarized π -system in the excited state than in the ground state (Figure 4 and S25).

All three dyes show quite large Stokes shifts, ranging from 41 nm (2427 cm^{-1}) (O_2 in cyclohexane) to almost 190 nm (8310 cm^{-1}) (S_2 in acetonitrile) in relationship with the increasing polarity of the solvents indicating the charge transfer character of all three fluorophores.

The analyses of the photoluminescent properties in several solvents indicates how the substitution of chalcogen atoms influences the emission. O_2 emits in the blue region with maximum wavelength ranging from 432 nm in non-polar

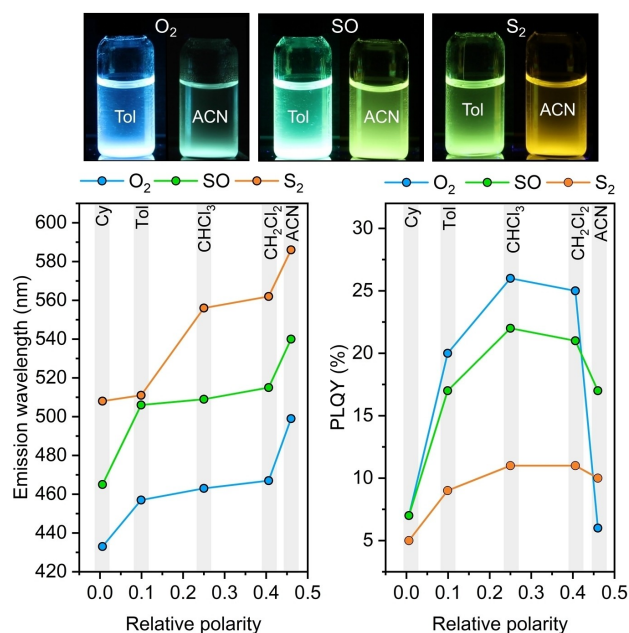


Figure 4. Top: Photographs of O₂, SO and S₂ in toluene (Tol) and acetonitrile (ACN). Under irradiation with a UV lamp ($\lambda_{\text{ex}} = 365$ nm). Bottom: Photo-luminescence quantum yields (PLQY) and emission wavelengths in dependency of the corresponding solvent polarity (Cy – Cyclohexane, Tol – toluene, CHCl₃ – chloroform, CH₂Cl₂ – dichloromethane, ACN – acetonitrile).

cyclohexane up to 513 nm in *N,N'*-dimethylformamide (DMF). Noteworthy, in DMF the emission is very weak and almost no detectable with naked eyes. The Φ_{PL} is low in cyclohexane as well as in high polar solvents such as acetonitrile (ACN), whereas an intense emission was observed in solvents with middle range polarity, such as chloroform and DCM, with a Φ_{PL} exceeding 20%. Upon gradual replacement of one oxygen atom by sulfur, SO exhibits emission from blue (465 nm in cyclohexane) to green-yellowish (540 nm in ACN) by increasing polarity of the solution, thus showing a similar trend to O₂. In contrast, the Φ_{PL} values in SO are high in all solvents, with a peak of 47% reached in DMF. Noteworthy, the k_r in DMF results were found to be two order of magnitude higher than in O₂, indicating that the radiative decay occurs more efficiently in the asymmetric compound (Table 1). The substitution of both oxygen atoms in S₂ shifts the emission further towards lower energy in all investigated solvents from green (508 nm in cyclohexane) to yellow (577 nm in ACN) (Figure 4). The good emission properties of S₂ are confirmed by the Φ_{PL} values, which are exceeding 10% in both polar and non-polar solvents, with the highest value recorded in DMF (30%). Noteworthy, in DMF the lifetime is the longest among the three dyes (also considering the six studied solvents) resulting in the lowest deactivation rate k_{nr} . Interestingly, the three fluorophores show a double exponential radiative decay only in DMF, suggesting the presence of two different coordination species. Indeed, the emission bands in DMF show a shoulder at higher energy.

Molecular quantum chemical simulations

The geometries of the three compounds were optimized at their electronic ground state (GS) and first bright state using Gaussian 16 program.^[34] Geometry optimizations were performed with two DFT functionals: (1) a hybrid functional B3LYP^[35] with Grimme-D3(BJ) dispersion correction; (2) range-separated hybrid functional ω B97^[36] with Grimme-D3 dispersion correction. In both cases the 6-311G* basis set was used.

The vertical excitation energies (VEEs) were calculated for DFT-based geometries at two levels of theory: CC2^[37] and ADC(2)/cc-pVTZ.^[38] Both methods were used in the resolution-of-the-identity (RI) formulation. The cc-pVTZ basis set and the corresponding auxiliary basis set were used. The calculated VEEs based on the ground state optimized geometries were compared to the experimental λ_{max}^a values while those based on the excited state optimized geometries were compared to λ_{max}^a values. The solvent effects were taken into account by a continuum solvation model.^[39] The Turbomole V7.3 program was used for these simulations.^[40]

The ground state optimized geometries show an increase of the bending with stepwise substitution of oxygen by sulfur atoms. While O₂ is planar, SO has a 138° and S₂ has 127° angle between the two terminal rings (Figure S21). It indicates that the sulfur containing compounds are already bent in solution, which means it is not only a property of solid-state packing in the crystal. We can rationalize the differences between these angles by relating to the 2s orbital the oxygen atoms that has only one radial node, so its radial distribution function (RDF) peaks farther away from the nucleus than in the case of 1s counterpart. Contrarily, the 2p orbitals have no radial nodes and hence their RDF peak is relatively close to the 2s function. Despite their energy gaps, this formally supports potential sp hybridization and bonding angles above 100°. In sulfur, however, the 3s and 3p orbital have two and one radial nodes, respectively, and hence the 3p functions dominate the chemical bonding and angles at around 90°.

In all three compounds the first excited state is the spectroscopic bright state, which has the major contribution from HOMO-LUMO. The experimental trend for example in DCM solution (Table 1) 390 nm (O₂), 411 nm (SO) and 395 nm (S₂) is reproduced. The calculated VVEs for O₂, SO and S₂ are found to be shifted hypsochromically in all the calculations. We attribute it to the small variation in absorption maxima of 21 nm found experimentally. This small difference can be explained by inspection of the HOMO and LUMO. The extension of the HOMO over the entire aromatic framework and a localisation of the LUMO on the dicyanobenzene moiety reveals some partial charge-transfer nature of the excitation.

The HOMO is the electron donor and the LUMO the electron acceptor with a HOMO-LUMO overlap restricted to the dicyanobenzene. The LUMO does not extend to the bridge and therefore it is not affected by the bending (Figure 5).

Similarly, the VEEs for the excited state were calculated to estimate λ_{max} for the emission spectra and were found to represent the experimental trend well (Table S5 and S9). In DCM the following trend is observed experimentally: 467 nm

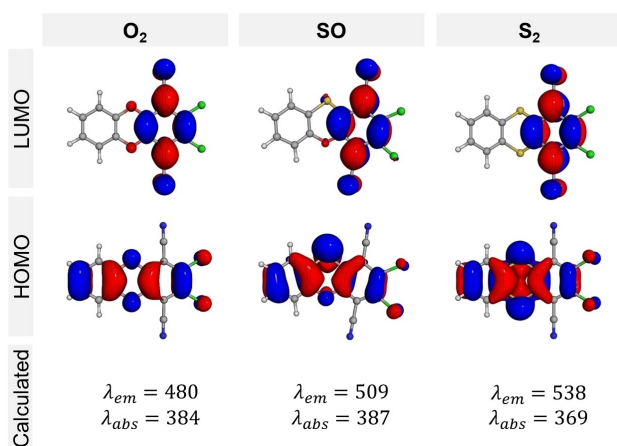


Figure 5. Calculated excitation energies of (O₂), (SO) and (S₂) at the RI-CC2/cc-pVTZ level of theory. The corresponding HOMO and LUMO as well as the absorption/emission wavelengths are shown.

(O₂), 515 nm (SO) and 562 nm (S₂). The computed counterparts at the CC2 level of theory are 480 nm (O₂), 509 nm (SO) and 538 nm (S₂). Hence, the measured Stokes shifts are 74 nm (4089 cm⁻¹) (O₂), 103 nm (4876 cm⁻¹) (SO) and 168 nm (7554 cm⁻¹) (S₂), whereas the calculated Stokes shifts are 96 nm (5208 cm⁻¹) (O₂), 122 nm (6193 cm⁻¹) (SO) and 169 nm (8513 cm⁻¹) (S₂).

The increase of the Stokes shift correlates well with the geometrical changes upon relaxation in the excited state.

This can be measured by change in the bending angle which is denoted by Δ in Figure 6. For SO and S₂ the geometry is relatively more planar in the S₁ state compared to S₀.

Emission behaviour in the aggregated and solid-state

The analyses of the photophysical properties as aggregates and solid states reveal more information about the structure-property relationship for the three fluorophores.

Interestingly, all three compounds show SSSE behaviour with an intense emission (Table 1, S12 and Figure S26) as bulk powder. In the solid-state the dyes show a trend similar to the solution, i.e., a bathochromic shift of the emission upon

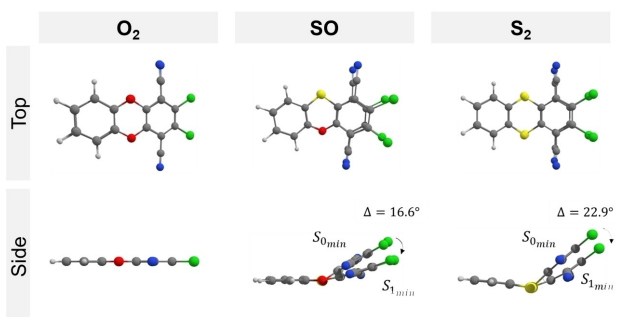


Figure 6. Differences in the bending angle between the two terminal rings in the relaxed ground state and excited state geometry. For every compound, the change in the bending angle is denoted with Δ .

gradual substitution of oxygen with sulfur (464 nm, 516 nm and 556 nm for O₂, SO and S₂, respectively). The efficiency Φ_{PL} of the oxygen-containing dyes has almost the same value (16 % for O₂, and 14 % for SO), whereas is dramatically increased after the removal of oxygen content in S₂ (40%) (Table 1). Notably, in solid state S₂ shows long-lived phosphorescence emission with lifetime of hundreds of microseconds (Figure S26), which is in agreement with the behaviour observed in other luminogens with high content of sulfur.^[41]

The nearly equally emissive properties in solution as well as in the solid-state, which is rarely reported in literature, suggests that the designed molecules suppress efficiently the vibrational and rotational motion in both environments. In particular, the reported synthetic approach based on the formation of condensed aromatic structures reduces the number of non-radiative processes in both solution and solid state. Indeed, the presence of free-rotational rings inside the dyes is known to be an effective deactivation pathway of the emission. As consequence, our study underlines one more time the importance of using condensed heterocycle aromatic systems to obtain efficient SSSE dyes.

It is worth to emphasize that the use of different chalcogens allows emission tuning and also the behaviour in the aggregate form, as it appears clearly from Figure 7 and S27. O₂ in DMF is almost not emitting, but by increasing the content of water the phenomenon of AIE occurs with a hypsochromic shift of the emission band from faint greenish to blue. In contrast, under the same conditions S₂ seems to show the opposite behaviour, i.e., aggregation-caused quenching (ACQ) phenomenon.

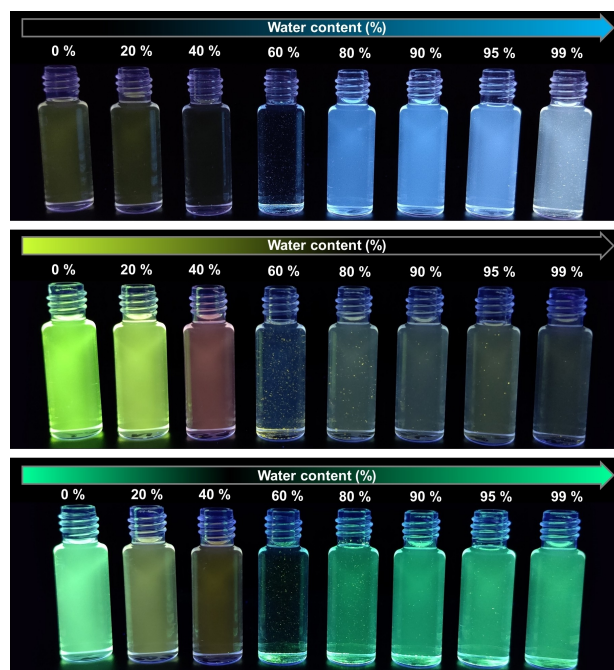


Figure 7. Photographs under UV light ($\lambda_{ex} = 365$ nm) of O₂ (top row), S₂ (middle row) and SO (bottom row) in DMF with increasing water content (0–99%).

However, a deep analysis reveals an unusual behaviour. The intense yellow colour in DMF disappears by enhancing the amount of water, whereas the presence of two emitting species became more evident by the splitting of the emission band.

The lower energy component (corresponding to the highest emitting species) shows ACQ, while the other slightly increases as AIE. (Figure S27, Table S13–S15). Interestingly, **SO** exhibits an intermediate behaviour. The red-shifted emission occurring with the ACQ change into AIE if the content of water is higher than 60 %.

Conclusion

In summary, we described a set of three simple highly emissive compounds based on bridged halogenated ethers with chalcogen variation. It was found that the content of sulfur influences the photophysical properties drastically, leading to a remarkable red-shift upon sulfur content increase. The experimental results were supported by DFT based simulations, X-ray diffractometric analyses as well as Hirshfeld investigations. The most important outcome is the fine tuning abilities of the emission behaviour in the aggregated state. Here, we were able to tune the emission properties of the three compounds in the molecularly dissolved state (DMF) and as aggregates (H₂O) by subtle structural changes, which will for sure open novel avenues for the design and application of luminophores sensitive to the state of aggregation.

Acknowledgements

JV, JD and FR thank the Deutsche Forschungsgemeinschaft (DFG) – (Grant: VO 2383/1-1, project number: 405679982, to JV, RI 2635/6-1, project number: 464509280 to FR) for funding. I.S. and O.F. acknowledge funding by the Deutsche Forschungsgemeinschaft (DFG, German Research Foundation) – Project-ID 221545957 – SFB 1078/C6. Additionally Steffen Riebe and Harini Hemesh are acknowledged for experiments conducted in the initial phase of the project and growing of the single crystals. We thank the Center for Nanointegration Duisburg-Essen (CENIDE) for financial support. Open Access funding enabled and organized by Projekt DEAL.

Conflict of Interest

The authors declare no conflict of interest.

Data Availability Statement

The data that support the findings of this study are available from the corresponding author upon reasonable request.

Keywords: aggregation · aggregation-induced emission · chalcogens · computational chemistry · solid-state structures

- [1] a) L. Basabe-Desmonts, D. N. Reinhoudt, M. Crego-Calama, *Chem. Soc. Rev.* **2007**, *36*, 993–1017; b) D. Chen, C. Liu, J. Tang, L. Luo, G. Yu, *Polym. Chem.* **2019**, *10*, 1168–1181; c) H. Wang, X. Ji, Z. A. Page, J. L. Sessler, *Mater. Chem. Front.* **2020**, *4*, 1024–1039.
- [2] a) T. Nagano, *Proc. Jpn. Acad. Ser. B* **2010**, *86*, 837–847; b) T. Terai, T. Nagano, *Pfluegers Arch.* **2013**, *465*, 347–359; c) L. Gao, W. Wang, X. Wang, F. Yang, L. Xie, J. Shen, M. A. Brimble, Q. Xiao, S. Q. Yao, *Chem. Soc. Rev.* **2021**, *50*, 1219–1250.
- [3] a) J. Mei, N. L. C. Leung, R. T. K. Kwok, J. W. Y. Lam, B. Z. Tang, *Chem. Rev.* **2015**, *115*, 11718–11940; b) J. Grolleau, R. Petrov, M. Allain, W. G. Skene, P. Frère, *ACS Omega* **2018**, *3*, 18542–18552; c) M. Hayduk, S. Riebe, J. Voskuhl, *Chem. Eur. J.* **2018**, *24*, 12221–12230; d) F. Würthner, *Angew. Chem. Int. Ed.* **2020**, *59*, 14192–14196; *Angew. Chem.* **2020**, *132*, 14296–14301.
- [4] B. Andreiuk, A. Reisch, E. Bernhardt, A. S. Klymchenko, *Chem. Asian J.* **2019**, *14*, 836–846.
- [5] S. Feng, S. Gong, G. Feng, *Chem. Commun.* **2020**, *56*, 2511–2513.
- [6] Y. Huang, J. Xing, Q. Gong, L.-C. Chen, G. Liu, C. Yao, Z. Wang, H.-L. Zhang, Z. Chen, Q. Zhang, *Nat. Commun.* **2019**, *10*, 169.
- [7] a) N. L. C. Leung, N. Xie, W. Yuan, Y. Liu, Q. Wu, Q. Peng, Q. Miao, J. W. Y. Lam, B. Z. Tang, *Chem. Eur. J.* **2014**, *20*, 15349–15353; b) Y. Tu, Z. Zhao, J. W. Y. Lam, B. Z. Tang, *Natl. Sci. Rev.* **2021**, *8*, nwa260.
- [8] G. C. Schmidt, *Ann. Phys.* **1921**, *370*, 247–256.
- [9] J. Luo, Z. Xie, J. W. Y. Lam, L. Cheng, H. Chen, C. Qiu, H. S. Kwok, X. Zhan, Y. Liu, D. Zhu, B. Z. Tang, *Chem. Commun.* **2001**, 1740–1741.
- [10] Y. Chen, J. W. Y. Lam, R. T. K. Kwok, B. Liu, B. Z. Tang, *Mater. Horiz.* **2019**, *6*, 428–433.
- [11] Z. Li, X. Ji, H. Xie, B. Z. Tang, *Adv. Mater.* **2021**, *33*, 2100021.
- [12] Q. Peng, L. Yang, Y. Li, Y. Zhang, T. Li, Y. Qin, Y. Song, H. Hou, K. Li, *J. Phys. Chem. C* **2020**, *124*, 22684–22691.
- [13] S. Xie, A. Y. H. Wong, S. Chen, B. Z. Tang, *Chem. Eur. J.* **2019**, *25*, 5824–5847.
- [14] R. Zhan, Y. Pan, P. N. Manghnani, B. Liu, *Macromol. Biosci.* **2017**, *17*, 1600433.
- [15] H. Li, H. Kim, J. Han, V.-N. Nguyen, X. Peng, J. Yoon, *Aggregate* **2021**, *2*, e51.
- [16] X. Zhai, R. Chen, W. Shen, *TrAC Trends Anal. Chem.* **2022**, *146*, 116502.
- [17] a) S. Majji, P. Alam, G. S. Kumar, S. Biswas, P. K. Sarkar, B. Das, I. Rehman, B. B. Das, N. R. Jana, I. R. Laskar, S. Acharya, *Small* **2017**, *13*, 1603780; b) H. Nie, B. Chen, J. Zeng, Y. Xiong, Z. Zhao, B. Z. Tang, *J. Mater. Chem. C* **2018**, *6*, 3690–3698.
- [18] S. Kumar, P. Singh, P. Kumar, R. Srivastava, S. K. Pal, S. Ghosh, *J. Phys. Chem. C* **2016**, *120*, 12723–12733.
- [19] a) A. Patra, S. P. Anthony, T. P. Radhakrishnan, *Adv. Funct. Mater.* **2007**, *17*, 2077–2084; b) J. Shi, N. Chang, C. Li, J. Mei, C. Deng, X. Luo, Z. Liu, Z. Bo, Y. Q. Dong, B. Z. Tang, *Chem. Commun.* **2012**, *48*, 10675–10677.
- [20] G. Chen, W. Li, T. Zhou, Q. Peng, D. Zhai, H. Li, W. Z. Yuan, Y. Zhang, B. Z. Tang, *Adv. Mater.* **2015**, *27*, 4496–4501.
- [21] J. L. Belmonte-Vázquez, Y. A. Amador-Sánchez, L. A. Rodríguez-Cortés, B. Rodríguez-Molina, *Chem. Mater.* **2021**, *33*, 7160–7184.
- [22] S. K. Behera, S. Y. Park, J. Gierschner, *Angew. Chem. Int. Ed.* **2021**, *60*, 22624–22638.
- [23] N. A. Kukhta, M. R. Bryce, *Mater. Horiz.* **2021**, *8*, 33–55.
- [24] S. Thulaseedharan Nair Sailaja, I. Maisuls, J. Kösters, A. Hepp, A. Faust, J. Voskuhl, C. A. Strassert, *Beilstein J. Org. Chem.* **2020**, *16*, 2960–2970.
- [25] W. Dai, P. Liu, S. Guo, Z. Liu, M. Wang, J. Shi, B. Tong, T. Liu, Z. Cai, Y. Dong, *ACS Appl. Bio Mater.* **2019**, *2*, 3686–3692.
- [26] N. Venkatramaiah, G. D. Kumar, Y. Chandrasekaran, R. Ganduri, S. Patil, *ACS Appl. Mater. Interfaces* **2018**, *10*, 3838–3847.
- [27] Y. Lei, Q. Liu, L. Dong, Z. Cai, J. Shi, J. Zhi, B. Tong, Y. Dong, *Chem. Eur. J.* **2018**, *24*, 14269–14274.
- [28] Y. Xu, H. Zhang, N. Zhang, X. Wang, D. Dang, X. Jing, D. Xi, Y. Hao, B. Z. Tang, L. Meng, *ACS Appl. Mater. Interfaces* **2020**, *12*, 6814–6826.
- [29] a) S. Riebe, C. Vallet, F. van der Vight, D. Gonzalez-Abadelo, C. Wölper, C. A. Strassert, G. Jansen, S. Knauer, J. Voskuhl, *Chem. Eur. J.* **2017**, *23*, 13660–13668; b) J. Stelzer, C. Vallet, A. Sowa, D. Gonzalez-Abadelo, S. Riebe, C. G. Daniliuc, M. Ehlers, C. A. Strassert, S. K. Knauer, J. Voskuhl, *ChemistrySelect* **2018**, *3*, 985–991; c) S. Riebe, C. Wölper, J. Balszuweit, M. Hayduk, M. E. Gutierrez Suburu, C. A. Strassert, N. L. Doltsinis, J. Voskuhl, *ChemPhotoChem* **2020**, *4*, 398–406.

- [30] S. Riebe, S. Adam, B. Roy, I. Maisuls, C. G. Daniliuc, J. Dubbert, C. A. Strasser, I. Schapiro, J. Voskuhl, *Chem. Asian J.* **2021**, *16*, 2307–2313.
- [31] a) J. Wang, Z. Liu, S. Yang, Y. Lin, Z. Lin, Q. Ling, *Chem. Eur. J.* **2018**, *24*, 322–326; b) W. Xi, J. Yu, M. Wei, Q. Qiu, P. Xu, Z. Qian, H. Feng, *Chem. Eur. J.* **2020**, *26*, 3733.
- [32] X. Ma, J. Cheng, J. Liu, X. Zhou, H. Xiang, *New J. Chem.* **2015**, *39*, 492–500.
- [33] P. R. Spackman, M. J. Turner, J. J. McKinnon, S. K. Wolff, D. J. Grimwood, D. Jayatilaka, M. A. Spackman, *J. Appl. Crystallogr.* **2021**, *54*, 1006–1011.
- [34] Gaussian 16, Rev. C.01, M. J. Frisch, G. W. Trucks, H. B. Schlegel, G. E. Scuseria, M. A. Robb, J. R. Cheeseman, G. Scalmani, V. Barone, G. A. Petersson, H. Nakatsuji, X. Li, M. Caricato, A. V. Marenich, J. Bloino, B. G. Janesko, R. Gomperts, B. Mennucci, H. P. Hratchian, J. V. Ortiz, A. F. Izmaylov, J. L. Sonnenberg, D. Williams-Young, F. Ding, F. Lipparini, F. Egidi, J. Goings, B. Peng, A. Petrone, T. Henderson, D. Ranasinghe, V. G. Zakrzewski, J. Gao, N. Rega, G. Zheng, W. Liang, M. Hada, M. Ehara, K. Toyota, R. Fukuda, J. Hasegawa, M. Ishida, T. Nakajima, Y. Honda, O. Kitao, H. Nakai, T. Vreven, K. Throssell, J. A. Montgomery, Jr., J. E. Peralta, F. Ogliaro, M. J. Bearpark, J. J. Heyd, E. N. Brothers, K. N. Kudin, V. N. Staroverov, T. A. Keith, R. Kobayashi, J. Normand, K. Raghavachari, A. P. Rendell, J. C. Burant, S. S. Iyengar, J. Tomasi, M. Cossi, J. M. Millam, M. Klene, C. Adamo, R. Cammi, J. W. Ochterski, R. L. Martin, K. Morokuma, O. Farkas, J. B. Foresman, D. J. Fox, Gaussian, Inc., Wallingford CT, **2016**.
- [35] A. D. Becke, *J. Chem. Phys.* **1993**, *98*, 5648–5652.
- [36] J.-D. Chai, M. Head-Gordon, *Phys. Chem. Chem. Phys.* **2008**, *10*, 6615–6620.
- [37] C. Hättig, F. Weigend, *J. Chem. Phys.* **2000**, *113*, 5154–5161.
- [38] C. Hättig in *Structure Optimizations for Excited States with Correlated Second-Order Methods: CC2 and ADC(2)*, Academic Press, **2005**, pp. 37–60.
- [39] A. Klamt, G. Schüürmann, *J. Chem. Soc. Perkin Trans. 2* **1993**, 799–805.
- [40] TURBOMOLE V7.2 **2017**, a development of University of Karlsruhe and Forschungszentrum Karlsruhe GmbH, 1989–2007, TURBOMOLE GmbH, since 2007; available from <http://www.turbomole.com>.
- [41] a) M. Hayduk, T. Schaller, F. C. Niemeyer, K. Rudolph, G. H. Clever, F. Rizzo, J. Voskuhl, *Chem. Eur. J.* **2022**, *28*, e202201081; b) M. Baroncini, G. Bergamini, P. Ceroni, *Chem. Commun.* **2017**, *53*, 2081–2093.
- [42] Deposition Number(s) **S₂** (2164566), **O₂** (2164859), **SO** (2164860) contain(s) the supplementary crystallographic data for this paper. These data are provided free of charge by the joint Cambridge Crystallographic Data Centre and Fachinformationszentrum Karlsruhe Access Structures service.

Manuscript received: June 23, 2022
Revised manuscript received: August 24, 2022
Accepted manuscript online: August 25, 2022
Version of record online: October 1, 2022